Fluid-Structure Interaction in Internal Physiological Flows

Matthias Heil and Andrew L. Hazel

School of Mathematics, University of Manchester, Manchester, M13 9PL United Kingdom; email: M.Heil@maths.man.ac.uk, Andrew.Hazel@manchester.ac.uk

Annu. Rev. Fluid Mech. 2011. 43:141–62

The *Annual Review of Fluid Mechanics* is online at fluid.annualreviews.org

This article's doi: 10.1146/annurev-fluid-122109-160703

0066-4189/11/0115-0141$20.00

Keywords

collapsible tubes, self-excited oscillations, phonation, pulmonary airway closure, pulmonary airway reopening

Abstract

We provide a selective review of recent progress in the analysis of several physiological and physiologically inspired fluid-structure interaction problems, our aim being to explain the underlying physical mechanisms that cause the observed behaviors. Specifically, we discuss recent studies of self-excited oscillations in collapsible tubes, focusing primarily on studies of an idealized model system, the Starling resistor—a device used in most laboratory experiments. We next review studies of a particular physiological, flow-induced oscillation: vocal-fold oscillations during phonation. Finally, we discuss the closure and reopening of pulmonary airways, physiological fluid-structure interaction problems that also involve the airways' liquid lining.

1. INTRODUCTION

Fluid-structure interaction plays an important role in many physiological phenomena throughout the human body. Examples include pulse-wave propagation in the arteries, flow-rate limitation and wheezing during forced expiration, pulmonary airway closure and reopening, phonation and snoring, the function of cardiac and venous valves, and the flow-induced deformation and ultimate rupture of arterial and cerebral aneurysms.

Here we present a selective review of recent studies concerning physiological and physiologically inspired fluid-structure-interaction problems. The selection of material reflects our own interests (and bias) but, in addition, we do not discuss topics recently reviewed either in this series or elsewhere. For instance, the dynamics of natural and artificial heart valves has been reviewed comprehensively by Dasi et al. (2009) and Weinberg et al. (2010). Other reviews discuss the growth and rupture of arterial and cerebral aneurysms (Humphrey & Taylor 2008, Lasheras 2007, Sforza et al. 2009), flow in the microcirculation (Popel & Johnson 2005), and pulse-wave propagation (van de Vosse & Stergiopulos 2011). The most recent general review of the subject by Grotberg & Jensen (2004) still provides a good overview of the field. Rather than reporting recent progress on every topic discussed in that paper, we instead focus on a more in-depth discussion of a smaller number of phenomena, focusing on progress in understanding the underlying physical mechanisms that cause particular behaviors.

Section 2 discusses recent progress in the study of self-excited oscillations in collapsible tubes, focusing primarily on studies of an idealized model system, the Starling resistor (a device used in most laboratory experiments of flow in collapsible tubes), rather than specific physiological applications. Section 3 continues the discussion of flow-induced oscillations but with a specific physiological example: vocal-fold oscillations during phonation. Finally, Section 4 is concerned with the effects of fluid-structure interaction in the pulmonary airways, in which the presence of the liquid lining and its associated surface tension plays an important role.

2. FLOW IN COLLAPSIBLE TUBES

Most fluid-conveying vessels in the human body are subject to a positive transmural (internal minus external) pressure, and accordingly they have an approximately circular cross section, minimizing their flow resistance. In this configuration the vessels are relatively stiff, and the fluid load induces only small deformations. However, if the vessels become subject to negative transmural pressures of sufficient magnitude, they can buckle nonaxisymmetrically. In this configuration a vessel's stiffness is dominated by its relatively small resistance to bending, and even small variations in the internal fluid pressure induce large changes in wall shape—a strong fluid-structure interaction. An intriguing feature of this system is that nonaxisymmetrically collapsed vessels readily develop flow-induced, self-excited oscillations. Physiological examples include wheezing during forced expiration, the development of Korottkoff sounds during sphygmomanometry, and cervical venous hum, generated by oscillations of the external jugular vein. We refer readers to Heil & Jensen (2003) and Grotberg & Jensen (2004) for a more comprehensive review of collapsible-tube phenomena in physiology.

Oscillations in collapsible tubes are examined experimentally by using a Starling resistor, sketched in **Figure 1*a***, in which flow is driven through a thin-walled elastic tube mounted on two rigid tubes and enclosed in a pressure chamber. This system and its two-dimensional (2D) equivalent, shown in **Figure 1*b***, have become canonical model problems for the analysis of flow-induced oscillations in collapsible tubes and are the focus of most of the studies reviewed below.

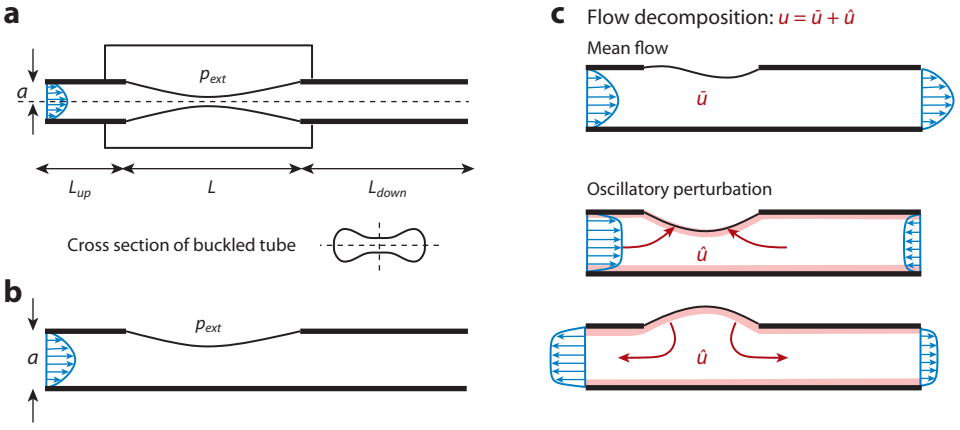

Figure 1

(*a*) Sketch of the Starling resistor, a thin-walled elastic tube, mounted on two rigid tubes, and enclosed in a pressure chamber, and (*b*) its 2D equivalent, a channel in which part of one wall is replaced by a prestressed elastic membrane. (*c*) Illustration of the sloshing mechanism. The flow is decomposed into its mean and oscillatory components, $\bar{\mathbf{u}}$ and $\hat{\mathbf{u}}$, respectively. The wall motion creates oscillatory sloshing flows in the upstream and downstream rigid sections. At sufficiently high frequency, the sloshing flows have a blunt inviscid core, with thin Stokes layers near the walls.

Early collapsible-tube experiments, reviewed in Bertram (2003), identified a large number of different types of oscillations, ranging from high-frequency flutter to low-frequency milking. However, the mechanisms responsible for the onset of these oscillations remain poorly understood; in particular, it remains unclear whether they are related to flow-induced instabilities, such as the traveling-wave-flutter or static-divergence mechanisms that successfully explain the onset of instabilities in other fluid-elastic systems (see, e.g., Carpenter & Garrad 1985, 1986).

Most early theoretical analyses of flow in the Starling resistor were based on lumped-parameter or spatially 1D models (reviewed in Heil & Jensen 2003, Pedley & Luo 1998). Such models are still widely used to describe networks of collapsible tubes, e.g., Bull et al.'s (2005) study of flow limitation in liquid-filled lungs; Fullana & Zaleski's (2009) analyses of flow in the venous network; and Venugopal et al.'s (2009) investigations of the lymphatic system, in which the collapsible vessels' stiffnesses are adjusted to simulate active pumping. The relative simplicity of these models facilitates rigorous mathematical analysis, which often aids the identification of mechanisms that explain the systems' behavior. However, a shortcoming of this approach is the need to provide closure assumptions, e.g., to capture the effects of viscous dissipation within the framework of a 1D, cross-sectionally averaged flow model, or to represent the 3D wall mechanics in terms of a so-called tube law: a postulated functional relationship between the vessel's cross-sectional area and the local transmural pressure. Results obtained from models involving such closure assumptions must be treated with caution. Indeed, many models of flow in the Starling resistor that used plausible, but nonetheless ad hoc, closure relations were able to predict the occurrence of self-excited oscillations, despite the fact that the underlying assumptions were later discredited. For instance, Cancelli & Pedley's (1985) widely used assumption that the majority of the viscous dissipation arises in the separated-flow region downstream of the tube's most strongly collapsed cross section (the throat) was found to be unsupported when subsequent Navier-Stokes simulations by Luo & Pedley (1996) showed that most of the dissipation arises in boundary layers on the upstream tube walls.

The introduction of closure assumptions can be avoided by modeling the system using the equations of continuum mechanics, for instance, the Navier-Stokes equations coupled to large-displacement elasticity theory. These equations provide a common starting point for direct numerical simulations and for the development of rational theoretical models, i.e., models in which the mechanics is described using rigorous (asymptotic) simplifications of the governing equations. A successful example of the latter approach is given by Whittaker et al. (2010b) who derived a tube-law-like description of the wall mechanics from the equations of Kirchhoff-Love shell theory without having to invoke any ad hoc assumptions.

2.1. Theoretical Studies

Many Navier-Stokes-based simulations of flow in the Starling resistor have considered flows in the 2D collapsible channel sketched in **Figure 1*b***. In this system the wall stiffness is dominated by the axial tension. If the tension is sufficiently small, the viscous pressure drop along the channel induces large-amplitude, steady wall deformations. In the absence of wall inertia, the steady configurations become unstable to relatively low-frequency self-excited oscillations when the Reynolds number is increased (Liu et al. 2009, Luo & Pedley 1996, Luo et al. 2008b). During the oscillation, so-called vorticity waves can develop downstream of the oscillating wall segment. These waves have also been observed in channels with a prescribed wall motion (Pedley & Stephanoff 1985; see also Rosenfeld 1995), so it is not clear whether they represent a passive fluid-mechanical response to the wall oscillation or play an active role in the mechanism responsible for its onset.

A systematic analysis of the system's linear stability in the absence of prestress (Luo et al. 2008b) reveals a cascade structure of instabilities: As the stiffness of the wall is reduced, the system can become unstable to perturbations of increasing axial wave number and frequency, each with different instability tongues, a feature also observed in some 1D models. Because the instabilities develop from strongly collapsed steady configurations, it is difficult to describe them in terms of a simplified theory. As a result, the mechanism(s) responsible for their onset, and whether those mechanism(s) could operate in three dimensions, remains unclear.

In contrast, much recent research has focused on a surprisingly simple instability mechanism, initially identified by Jensen & Heil (2003), that can operate in two and three dimensions when the wall stiffness is sufficiently large. In this regime, the steady viscous pressure drop induces only small wall deflections, and the oscillations (governed by a dynamic balance between fluid inertia and the large elastic restoring forces) are of high frequency.

The oscillatory wall motion periodically displaces fluid from the collapsible section into the rigid sections, as shown in **Figure 1*c***. If the amplitude of the resulting sloshing flows is greater in the rigid upstream section than in its downstream counterpart, then there is a net influx of kinetic energy into the system. If this influx exceeds any additional losses, the system can extract energy from the mean flow, and the amplitude of the oscillations grows. For the 2D model, Jensen & Heil (2003) employed asymptotic techniques to provide explicit predictions for the frequency and growth rates of instabilities arising through this mechanism, in the limit of large wall tension (or, equivalently, high frequency). Assuming the flow is driven by a prescribed pressure drop, they showed that the required upstream/downstream asymmetry of the sloshing flows can be generated by making the rigid downstream section longer than its upstream counterpart. The theoretical predictions for the critical Reynolds number at which oscillations develop were found to be in excellent agreement with results from direct numerical simulations, even in cases in which the tension was relatively small and the system performed oscillations of modest frequency.

In three dimensions, small-amplitude, nonaxisymmetric oscillations of an elastic tube about its axisymmetric equilibrium configuration create axial sloshing flows that are much weaker than their

2D equivalents. The induced unsteady flows are dominated by transverse flow within each cross section (Heil & Waters 2006), and there is little interaction with the mean flow. By analyzing the system's energy budget for prescribed wall motions, Heil & Waters (2008) and Whittaker et al. (2010c) showed that efficient extraction of energy from the mean flow via the sloshing mechanism requires the tube to perform oscillations about a nonaxisymmetric mean configuration. Thus, the instability is most likely to operate when oscillations arise from steady states in which either (*a*) the tube's undeformed cross sections are noncircular or (*b*) an initially axisymmetric tube has already buckled nonaxisymmetrically. These findings are consistent with experimental observations showing that self-excited oscillations tend to develop most readily from steady-state configurations in which the tube is strongly buckled (Bertram 2008).

Scenario (*a*) was investigated by Whittaker et al. (2010a), who combined an asymptotic description of the flow in rapidly oscillating collapsible tubes (Whittaker et al. 2010c) with a rational, tube-law-like description of the wall mechanics (Whittaker et al. 2010b) to derive explicit predictions for the onset of self-excited oscillations. For flows in elliptical tubes, these were found to be in good agreement with the results of direct numerical simulations. The existence of self-excited oscillations arising from the sloshing mechanism in scenario (*b*) was confirmed by Heil & Boyle (2010), who performed numerical simulations of flows in initially axisymmetric elastic tubes. For sufficiently long tubes, the growing oscillations ultimately settle into a large-amplitude limit cycle during which the tube shape alternates between two extreme configurations in which the major and minor half axes of the cross section are interchanged, similar to the classical shell mode oscillation observed in Weaver & Païdoussis's (1977) experiments.

The studies referred to above treat the onset of self-excited oscillations as a global stability problem and assess the stability of steady states by determining the frequency and growth rates of small-amplitude perturbations to the steady flow in a finite domain. An alternative approach is to consider the problem within the framework of a local stability analysis, more commonly used to investigate flow-induced instabilities in infinite domains via the dispersion relation for traveling-wave-type perturbations (see, e.g., Davies 2003, Hoepffner et al. 2010). Doare & de Langre (2004, 2006) showed that in 1D fluid-elastic systems, global instabilities in finite domains can be interpreted in terms of local modes that propagate within the domain and are reflected at its upstream and downstream boundaries. Stewart et al. (2009) adapted these methods to analyze self-excited collapsible-tube oscillations, initially using a 1D model of the Starling resistor. The approach was later extended to two dimensions (Stewart et al. 2010) by combining local eigenmodes of an Orr-Sommerfeld-like equation to describe perturbations to the steady mean flows in the three sections of a collapsible channel, using an approach developed by Manuilovich (2004). [The extension of this approach to three dimensions has not yet been considered, but the traveling-wave-type instabilities found in infinitely long 3D tubes, reviewed in Kumaran (2003), and particularly the analysis of nonaxisymmetric instabilities in such systems (Shankar & Kumaran 2000), are likely to provide a suitable framework for the description of the relevant local modes.]

Although the representation of the flow field in terms of local modes does not yield a particularly efficient computational method, Stewart et al. (2010) found the flow field computed with only a small number of local modes to be in good agreement with full numerical simulations. More importantly, the modal representation permits an assessment of the relative importance of the various local modes, many of which are well understood from previous studies. In particular, the approach can distinguish between hydrodynamic modes (such as Tollmien-Schlichting waves, modified by the presence of the wall elasticity) and modes that arise as a result of the wall elasticity, such as traveling-wave flutter and static divergence. In terms of these modes, Stewart et al. (2010) were able to interpret the high-frequency sloshing mechanism as a consequence of wave reflections of static divergence and traveling-wave-flutter modes at the junctions with the rigid channel

segments. A reduction in wall tension reduces the frequency of the oscillations and excites a convectively unstable traveling-wave-flutter mode. At even lower tensions, wave-like flow features begin to appear in the downstream rigid section via the excitation of hydrodynamic modes. [Although it is tempting to interpret these features as the equivalents of the vorticity waves mentioned above, the waves observed by Stewart et al. (2010) decay much more quickly than those in Luo et al.'s computations.] An analysis of the system's energy budget suggests that at low frequencies, the dominant source of energy responsible for the growth of the oscillations switches from the influx of kinetic energy (the signature of the sloshing mechanism) to a reduction in the total viscous dissipation in the flow, indicating that the oscillations are governed by a different mechanism.

LU/LD-type oscillations: two distinct types of large-amplitude low-frequency (L) oscillations observed in a collapsible tube; the tube is open/collapsed for the majority of the period so that its cross-sectional area remains near its maximum (up)/minimum (down)

A reduction in wall tension also affects the character of the system's large-amplitude limit-cycle oscillations. At large tensions, the wall performs approximately harmonic, large-amplitude oscillations in a mode shape that resembles the system's linear eigenmode (Jensen & Heil 2003). At lower tensions the system was found to perform what Stewart et al. (2010) termed "slamming oscillations," initially predicted by Stewart et al.'s (2009) 1D model and subsequently confirmed in 2D Navier-Stokes-based simulations. During these oscillations the collapsible segment experiences short phases of strong collapse near its downstream end, reminiscent of experimentally observed LU-type oscillations, which we discuss in the next section. So far, there have not been any theoretical or computational studies of these oscillations in the 3D system.

2.2. Experimental Studies

Early collapsible-tube experiments, reviewed in Bertram (2003), tended to concentrate on the classification of the system's sustained large-amplitude oscillations, in terms of macroscopic flow variables (flow rate and pressure variations) and their dependence on the system parameters. Much recent experimental work has focused on the visualization of the flow fields and the study of the onset of self-excited oscillations in a parameter regime in which the collapsible tube develops LU-type oscillations (Bertram et al. 1990). These studies have shown that during this particular type of oscillation, the two-lobed collapse of the tube creates two jet-like flow structures in the plane of the tube's major axis. The jets impinge on the tube wall near the downstream end of the collapsible segment, and the impact creates two sickle-shaped (and sometimes complete annular) regions of elevated axial velocity before the jets merge further downstream. A region of retrograde flow develops near the tube's centerline whenever the tube is sufficiently strongly collapsed. These flow features are remarkably robust and have been observed over a large range of Reynolds numbers, ranging from laminar flows at $Re \approx 300$ (Bertram et al. 2008) to fully turbulent flows at $Re \approx 10{,}000$ (Bertram & Nugent 2005). Furthermore, the oscillation frequency is relatively low, and these flow features are similar to those in steadily collapsed elastic (or rigid) tubes (Bertram & Godbole 1997, Bertram et al. 2001, Hazel & Heil 2003a, Marzo et al. 2005), suggesting that, for the type of oscillations considered here, the flow in the oscillating collapsible tube may be thought of as quasi-steady. Flow visualization inside the oscillating collapsible segment is challenging (Bertram et al. 2007, Burgmann et al. 2009, Ohba et al. 1997). However, the time traces of the volume flux in the upstream and downstream rigid segments already suffice to show that the largest fluctuations in flow rate typically occur downstream of the collapsible segment while the flow rate at the inflow remains approximately constant (Truong & Bertram 2009), indicating that the oscillations cannot be driven by the sloshing mechanism discussed above.

For sufficiently thin-walled tubes, self-excited LU-type oscillations can develop at Reynolds numbers as low as ≈250, with a maximum frequency of approximately 10 Hz. Bertram & Tscherry (2006) reported that the frequency of the oscillations decreases with an increase in the length of the downstream rigid tube, L_{down} (see also Wang et al. 2009), whereas a change in L_{down} does

not affect the Reynolds number at which the oscillations first develop. The oscillations have small Strouhal numbers, consistent with the assumption that the flow induced by the tube oscillation can be regarded as quasi-steady, but visualization of the flow downstream of the oscillating collapsible segment shows clear evidence of secondary shear-layer instabilities with much higher frequency than the tube oscillations (Truong & Bertram 2009). Although these shear-layer instabilities may not play a direct role in the mechanism responsible for the onset of the oscillations, accurate numerical simulation of the phenomenon will require such features to be resolved.

It is important to stress that the experiments referred to above only describe one particular type of oscillation; other types of oscillation have been observed at similar Reynolds numbers. For instance, flow visualizations by Ohba et al. (1997) show a single, central jet downstream of the collapsible segment, and experiments by Kounanis & Mathioulakis (1999) suggest that the onset of self-excited oscillations may be associated with symmetry breaking of the flow downstream of the throat.

2.3. Outlook

Despite the significant progress made in recent years, we do not yet have the ideal situation in which a conceptually simple instability mechanism that lends itself to a rational theoretical description (such as the sloshing mechanism) is confirmed by experiments. Estimates provided by Heil & Boyle (2010) and Whittaker et al. (2010a) suggest that it should be possible to modify existing collapsible-tube experiments (e.g., by changing the lengths of the upstream and downstream rigid pipes, or by driving the flow with a volumetric pump, attached to the downstream rigid tube) so that the accessible parameter regime is one in which the sloshing mechanism operates. However, such experiments have not yet been attempted.

Equally, there is no theoretical explanation for the instability characterized in the detailed experimental studies discussed above. Even though the experiments were performed at Reynolds numbers at which direct numerical simulations are feasible, simulations by themselves are unlikely to be able to reveal the underlying mechanism(s). The development of rational theoretical models for the onset of oscillations from strongly collapsed equilibrium configurations is likely to remain difficult because the base flow itself is not easy to describe in a simplified form, on account of the flow separation downstream of the throat. However, insight into the flow features gained from numerical simulations or flow visualizations could lead to the development of nonrational, but nevertheless useful, theoretical models to aid the identification of potential instability mechanisms.

The theoretical models reviewed above have generally ignored the effects of wall inertia, because its inclusion is not necessary to explain the onset of the flow-induced instabilities considered here. We stress, however, that the presence of wall inertia introduces additional modes of instability (Larose & Grotberg 1997, Luo & Pedley 1998) and that it is of relevance in physiological applications in which the wall density is much greater than that of the fluid [e.g., in respiratory flows (Bertram 2008)]. In the next section, we discuss self-excited oscillations of the vocal cords during phonation, a phenomenon in which wall inertia is of crucial importance.

3. PHONATION: SELF-EXCITED OSCILLATIONS OF THE VOCAL CORDS

The human vocal cords are a pair of muscular folds located in the central section of the larynx known as the glottis (see **Figure 2*a***). The position and shape of the folds can be actively controlled; for instance, during breathing the glottis tends to be fully open, but it can close completely when holding one's breath. When the folds are brought close together and the subglottal (upstream)

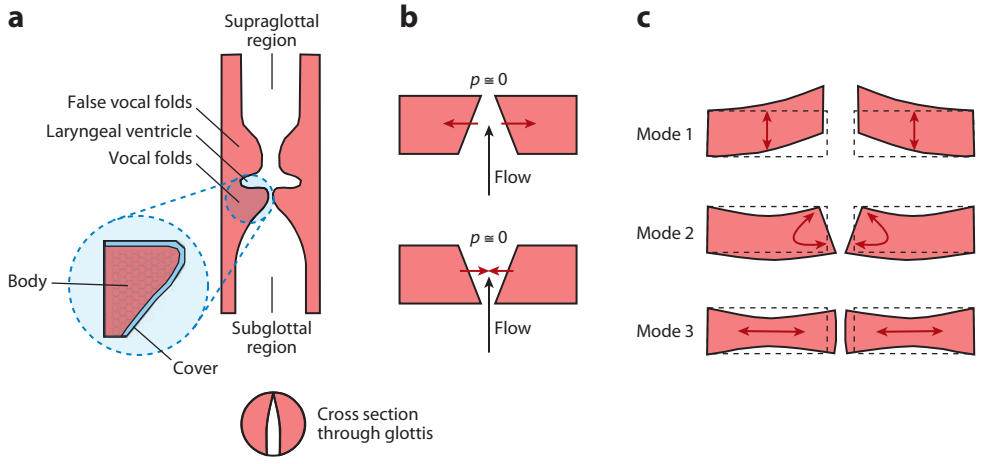

Figure 2

(*a*) Sketch of the larynx, showing the true and false vocal folds. The vocal folds have a complicated internal structure, here lumped into two main regions: the cover, which contains a highly flexible mucosal surface layer, and the body, which contains muscular fibers used to adjust the shape and tension of the vocal folds. (*b*) Sketch illustrating the changes to the vocal-fold geometry during oscillation, resulting in a convergent/divergent glottis when the vocal folds separate/approach each other. (*c*) Illustration of the vocal folds' three lowest-order in vacuo modes. The flow-induced synchronization and superposition of modes 2 and 3 can generate the vocal-fold oscillations shown in panel *b*.

pressure is increased beyond the so-called phonation-threshold pressure, air driven through the narrow gap can excite flow-induced oscillations that provide the main source of sound during speech and singing. The frequency of oscillation can be actively controlled by adjusting the folds' position, shape, and internal tension. Stroboscopic observations show the existence of several distinct types of oscillations, often associated with different vocal registers, such as the modal register used in normal speech and characterized by large-amplitude, low-frequency oscillations (approximately 100/200 Hz for males/females), during which the folds collide, or the falsetto register in which the folds are highly stretched and perform small-amplitude, high-frequency oscillations without contact. In this review our main focus is on oscillations in the modal register.

Using estimates based on the mean velocity and average glottal gap width, one finds that the flow through the glottis is of relatively high Reynolds number, $Re = \mathcal{O}(10^3)$, small Mach number, $Ma = \mathcal{O}(10^{-1})$, and small Strouhal number $St = \mathcal{O}(10^{-2})$ (Dejonckere & Lebacq 1981, Triep et al. 2005), which suggests that the basic mechanism responsible for the interaction between the vocal folds and the air flow is the Bernoulli effect: An increase in fluid velocity reduces the pressure between the folds and pulls them toward each other. The fluid velocity increases as the gap width decreases, and hence the vocal folds are pulled closer and closer together until they collide. The glottis then remains closed until the elastic recoil of the folds and a buildup of pressure upstream force them apart again.

Although the Bernoulli effect provides a destabilizing feedback between fluid and solid mechanics, it cannot explain the development of sustained oscillations in the presence of dissipation in the vocal-fold tissue. If the fluid forces were determined exclusively by the Bernoulli effect, with the fluid velocity set by the average cross-sectional area of the glottis, for example, the fluid pressure would always be in phase with the displacement and thus would not be able to perform any net work on the tissue. Titze (1988) identified two main mechanisms that have the potential to create a phase difference between pressure and displacement. (*a*) The acceleration and

deceleration of fluid in the vocal tract affect the fluid pressure at the glottis, an effect he referred to as "inertive vocal tract loading." (*b*) The vocal folds do not deform uniformly and adopt different shapes during different phases of the oscillation, which also affects the fluid load on the vocal fold. Excised larynxes are capable of producing sound, so the presence of the vocal tract cannot be a prerequisite for the development of oscillations, suggesting that the latter mechanism is more important. Indeed, high-speed visualization of the oscillating vocal folds shows that the narrowest part of the vocal folds tends to adopt a convergent (divergent) shape when the vocal folds move away from (toward) each other, as shown in **Figure 2*b***. Assuming that the pressure immediately downstream of the glottis remains constant, a reasonable assumption in the absence of the vocal tract, the steady Bernoulli equation shows that the pressure in the glottis increases (decreases) with the distance from its downstream end. Hence, the average fluid pressure acting on the vocal folds is larger when they separate than when they approach each other, allowing the fluid to perform work on the solid.

Empirical orthogonal eigenfunctions: provide a decomposition of a function of space and time, $\mathbf{u}(\mathbf{x}, t)$, in the form $\mathbf{u}(\mathbf{x}, t) = \bar{\mathbf{u}}(\mathbf{x}) + \sum_j U_j(t)\boldsymbol{\psi}_j(\mathbf{x})$, where $\bar{\mathbf{u}}(\mathbf{x})$ represents the temporal mean

Complete understanding of this deformation-based mechanism requires an explanation for the change in shape of the vocal folds during the oscillation. Early lumped-parameter models of this process (e.g., Ishizaka & Flanagan 1972, Titze 1973) allowed for variations in the cross-sectional area of the glottis by representing each vocal fold as pairs of transversely oscillating masses, loaded by the local fluid pressure. These models can exhibit vocal-fold oscillations of converging-diverging type and are able to predict the development of self-excited oscillations, but, as usual, the model parameters are difficult to relate to actual physiological measurements.

A continuum mechanical approach to the problem was introduced by Titze & Strong (1975), who suggested two alternative mechanisms to explain the periodic variation between converging/diverging glottis shapes: (*a*) surface waves that travel in the thin mucosal surface layer (McGowan 1991, Titze 1988) or (*b*) the macroscopic deformation of the entire vocal fold in its eigenmodes. Experiments with vocal-fold replicas have shown that either mechanism can lead to flow-induced oscillations by using replicas in which only the mucosal layer is elastic (Titze et al. 1995, Thomson et al. 2007) and others that are entirely made of an isotropic, homogeneous elastic material (Thomson et al. 2005). The eigenmode of a real, inhomogeneous vocal fold is therefore likely to incorporate contributions from both types of deformation.

Modeling the vocal folds as rectangular parallelepipeds with uniform elastic properties, Titze & Strong (1975) showed that the superposition of the system's three lowest-order in vacuo eigenmodes can create the appropriate periodic variation in glottis shapes, as shown in **Figure 2*c***. A tacit assumption required for this mechanism to apply is that the relevant in vacuo modes, each with its own distinct eigenfrequency, can be synchronized by their interaction with the fluid flow. Berry & Titze (1996) and Cook & Mongeau (2007) showed that the in vacuo frequencies of modes 2 and 3 are indeed very close over a wide range of constitutive parameters and geometries, suggesting that a weak interaction with the fluid flow may suffice to induce synchronization.

Empirical evidence that flow-induced synchronization of the in vacuo eigenmodes is involved in phonation is Kaneko et al.'s (1987) in vivo observation that, for a wide range of vocal-fold tensions, the phonation frequency tends to be close to the fundamental frequency of the folds' in vacuo oscillations. Additional support for the relevance of the vocal fold's in vacuo eigenfunctions was provided by Berry et al.'s (1994) and Alipour et al.'s (2000) numerical simulations of actual flow-induced oscillations. Both studies used more realistic representations of the vocal folds' geometry and structural properties, and coupled the deformation of the vocal folds to a fluid model that also incorporated the effect of the vocal tract. Berry et al. (1994) showed that the system's nonlinear oscillations, which involved nonlinearities due to the fluid loading and the collisions of the vocal folds, could be captured by a small number of empirical orthogonal eigenfunctions (Sirovich 1987) that were extracted from the numerical simulations. The lowest-order empirical

eigenfunctions were found to be similar to the folds' (linear) in vacuo eigenfunctions, and the nonlinearity of the self-excited oscillations manifested itself primarily in the nonharmonic time dependence of their amplitudes.

The mathematical framework for the description of instabilities arising via the synchronization of eigenmodes or mode coalescence is the theory of (strong) 1:1 resonance or Hamiltonian Hopf bifurcation (van der Meer 1990), strictly applicable only in undamped systems, and already known to Kelvin in the nineteenth century. Assuming that the system has been discretized and the discrete solid displacements are denoted by the vector $\mathbf{x}$, the small-amplitude in vacuo oscillations of the elastic body are governed by an equation of the form $\mathbf{M}\ddot{\mathbf{x}} + \mathbf{D}\dot{\mathbf{x}} + \mathbf{K}\mathbf{x} = \mathbf{0}$, where $\mathbf{M}$, $\mathbf{D}$, and $\mathbf{K}$ are real matrices. In the undamped case $\mathbf{D} = \mathbf{0}$, and assuming the normal form $\mathbf{x} = e^{\lambda t}\hat{\mathbf{x}}$ leads to the eigensystem $\lambda^2\mathbf{M}\hat{\mathbf{x}} + \mathbf{K}\hat{\mathbf{x}} = \mathbf{0}$. The eigenvalues must occur in complex conjugate pairs, and the system is neutrally stable if all the eigenvalues lie on the imaginary axis, in which case the imaginary part of the eigenvalue is the frequency of the corresponding neutral oscillations. Continuous changes in the system's parameters (e.g., via the influence of fluid loading) induce continuous changes in the spectrum, and the system becomes unstable when at least one eigenvalue has a positive real part, corresponding to exponential growth. In the Hamiltonian (undamped) system, this can only occur if a complex conjugate pair merges and separates along the real line, a static divergence instability, or if two complex conjugate pairs merge and move off the imaginary axis at a single frequency, the 1:1 resonance [see Mandre & Mahadevan (2010) for a simple example motivated by fluid-structure interaction]. The introduction of weak damping of various forms has been considered by many authors [see Krechetnikov & Marsden (2007) for a review and O'Reilly et al. (1996) for a general perturbation analysis]. The Hamiltonian Hopf bifurcation is now understood to be a singular limit of a codimension-3 dissipative normal form (Krechetnikov & Marsden 2007) with attendant complex dynamics. A generic possibility is that weak damping causes the two eigenvalue pairs that merged in the perfect system to pass near each other, but the direction of their motion in the complex plane can still change rapidly, whereas the frequencies of the two modes remain similar. The system's response to an eigenvalue crossing the imaginary axis will appear similar to a standard Hopf bifurcation in damped systems, but the underlying mechanism is fundamentally different because the crossing would not occur without the near interaction with another mode.

The synchronization of the vocal fold's in vacuo eigenmodes by the fluid flow was studied in detail by Zhang et al. (2007), who coupled a 2D linear elasticity model for the deformation of the vocal folds to a 1D potential flow model, initially assuming that flow separation always occurs at the downstream edge of the glottis. Zhang et al. (2007) showed that the coalescence of two in vacuo eigenmodes and the system's subsequent instability arise primarily through interaction induced by the Bernoulli effect, which manifests itself as a flow-induced stiffness. (Fluid mechanical effects that change the matrices $\mathbf{M}$, $\mathbf{D}$, and $\mathbf{K}$ are classified as providing flow-induced inertia, damping, and stiffness, respectively. The Bernoulli effect affects the stiffness because the fluid pressure depends on the local cross-sectional area, which is determined only by the displacement.)

Titze's (1988) assumption that the periodic variations in the glottis shape create the phase difference between fluid pressure and surface displacement that allows the fluid to perform work on the solid was confirmed by Thomson et al.'s (2005) detailed study of the energy transfer between the fluid and solid. Their fully coupled, fluid-structure-interaction simulations of vocal-fold oscillations also showed that the location of the point at which the flow separates from the walls of the diverging glottis has an important effect on the fluid pressure distribution and therefore on the energy transfer. This is consistent with the findings of Zhang (2008), who also showed that the phonation threshold pressure and the frequency of the oscillation depend sensitively on the initial shape of the glottis. This sensitivity forms a basis for laryngeal posturing—the active adjustment

of the shape and position of the vocal folds to control the frequency of their oscillation (see, e.g., Alipour & Scherer 2000, Hunter et al. 2004). Zhang (2009) recently observed that in certain parameter regimes, slight changes to the stiffness of the vocal-fold body can lead to drastic changes in the vocal-fold frequency and mode shape at phonation onset, reminiscent of a register change. Zhang (2009) showed that this was because phonation onset at large and small body stiffness was caused by the coalescence of different pairs of in vacuo eigenmodes in his model.

When performing sustained oscillations in the modal register, the vocal folds tend to collide, resulting in complete occlusion of the glottis for a significant fraction of the period of the oscillation. The collisions generate substantial impact stresses that can cause vocal trauma and are believed to be partly responsible for the development of vocal nodules. Experimental studies on excised canine larynxes by Jiang & Titze (1994) found an approximately linear relationship between the peak impact pressure and the subglottal (driving) pressure. This trend was also observed in Gunter's (2003) simulations of the in vacuo motion of spatially isotropic vocal folds. In subsequent simulations Tao et al. (2006) and Tao & Jiang (2007) investigated vocal-fold collisions in a fully coupled fluid-structure interaction model. Oscillations were found to develop via a supercritical Hopf bifurcation (which may in fact be a weakly dissipative Hamiltonian Hopf bifurcation, as discussed above) when the driving pressure, p_d, reached the phonation-threshold pressure, p_{pt}, with the amplitude of the oscillations then increasing with the square root of $(p_d - p_{pt})$. For driving pressures just in excess of p_{pt}, it was possible to obtain sustained oscillations without vocal-fold collisions; for larger values of p_d, regular collisions occurred, and the peak impact pressures increased approximately linearly with the amplitude of the vocal-fold oscillations.

The first of Titze's (1988) proposed mechanisms for the generation of a phase difference between pressure and displacement, inertive vocal tract loading, could not be assessed by the majority of the studies reviewed above because they focused on the flow in the immediate vicinity of the glottis. Recent immersed boundary computations that considered a larger region of the larynx have confirmed the importance of this effect (Luo et al. 2009) and provided further evidence for the onset of oscillations via synchronization of the fold's structural eigenmodes (Luo et al. 2008a). These studies also showed that the false vocal folds, ignored in most previous studies, with the notable exception of de Oliveira Rosa et al. (2003), have a strong effect on the flow field, which in turn affects the amplitude and frequency of the vocal-fold oscillation (Zheng et al. 2009a). The jet-like flow that emerged from the oscillating glottis was found to become asymmetric (due to the Coanda effect), and large-scale vortical flow structures developed further downstream. These observations are broadly consistent with those of many other studies that considered flows in rigid (e.g., Kucinschi et al. 2006) and oscillating vocal-fold replicas (e.g., Neubauer et al. 2007, Triep et al. 2005).

The flow field downstream of the vocal folds not only has a strong effect on their oscillations, but also plays an important role in the sound generation by aeroacoustic processes. As it is not possible to adequately review this literature here, we simply refer readers to papers by McGowan (1988) and Krane (2005) for a discussion of how the interaction of the vorticity with the vocal tract generates sound and mention that the first fully coupled simulations that involve fluid-structure interaction and aeroacoustics are becoming available (Link et al. 2009).

4. FREE-SURFACE FLUID-STRUCTURE INTERACTION PROBLEMS IN THE PULMONARY AIRWAYS

4.1. Airway Closure

Surface tension at the free surface between the thin liquid lining and the air-conveying core of the pulmonary airways contributes significantly to the overall stiffness of the lung and has a natural

tendency to collapse the airways (Macklem 1971). Such collapse can lead to airway closure in which alveolar gas exchange is impeded by fluid obstructions. At the time of writing, the evidence that airways close in vivo is indirect (Burger & Macklem 1968), but methods developed by Sera et al. (2008) for real-time imaging of rodent lungs in vivo may allow direct visualization of airway closure in the near future. The lung's propensity to closure increases with increasing fluid volume in the lung (e.g., in pulmonary edema), increasing surface tension (e.g., in neonatal respiratory distress syndrome), and/or reduction in the structural stiffness of the airways (e.g., in emphysema). Mechanical ventilation, or other treatments, of patients suffering from such conditions must ensure that blockages are removed as quickly as possible, but without causing damage to the lung.

Airway closure can be initiated by a surface-tension-driven instability (the Rayleigh-Plateau instability) that redistributes the airway's initially uniform liquid lining into an occluding liquid bridge (Johnson et al. 1991). The evolution of the instability and, hence, the likelihood of liquid-bridge formation are affected by wall elasticity, and Grotberg & Jensen (2004) reviewed initial studies of this process in which the airway deformations were constrained to remain axisymmetric or axially uniform. More recent studies, reviewed by Heil et al. (2008), have shown that the compressive load on the airway walls generated by the primary axisymmetric instability can induce axially nonuniform, nonaxisymmetric buckling. If the volume of fluid in the liquid lining is sufficiently large, buckling can be followed by a dramatic and extremely rapid collapse toward occlusion, after which the capillary-elastic system evolves toward a new static equilibrium: a locally deformed tube containing an occluding plug. For smaller fluid volumes, the liquid lining redistributes to form a nonoccluding collar or lobe without creating an occlusion. The final equilibrium attained depends on the precise details of the system's temporal evolution and on wall elasticity (Hazel & Heil 2005), tube curvature (Jensen 1997), gravity (Duclaux et al. 2006), and the contact angle between the interface and the tube wall (Lindsley et al. 2005), which can be nonzero because of interactions between surfactant, liquid, and wall surface molecules (Hills 1999, Yasuda et al. 1994). A complete characterization of the possible equilibria including all these physical effects remains an open problem.

4.2. Liquid Plug Propagation

Liquid plugs arise naturally in the pulmonary airways, as described above, and they are also deliberately introduced for drug-delivery applications, surfactant replacement therapy, or in partial liquid ventilation (Zheng et al. 2006). Both normal respiration and artificial ventilation impose a pressure drop across the liquid plug, which can initiate motion. Before propagation begins, a liquid film of finite thickness may be present on either side of the plug, and a steadily propagating state is then only possible if the mass of fluid deposited behind the advancing plug is equal to the mass accumulated ahead (Fujioka & Grotberg 2004, Howell et al. 2000). If the plug continually deposits more fluid than it accumulates, it will eventually rupture and the airway will reopen (Howell et al. 2000). In drug-delivery and surfactant-replacement therapies, early plug rupture will limit the efficacy of the treatment, which has motivated studies of the stability of steadily propagating plugs.

Considering plug propagation in rigid tubes, Campana et al. (2007) showed that for a given film thickness ahead of the plug, steady motion is only possible at a single propagation speed. They argued that the stability of these steadily propagating plugs can be inferred from steady calculations that determine the deposited film thickness, h, as a function of plug length, L_p. If $\partial h/\partial L_p > 0$ (<0), a quasi-steady decrease in plug length causes a decrease (increase) in the deposited film thickness, which increases (decreases) the plug length, so the steadily propagating plug is expected to be stable (unstable). The inferred stability was confirmed by studying the temporal evolution

of the system when either the propagation speed (Campana et al. 2007) or the driving pressure drop was held constant (Ubal et al. 2008). In the latter case, only relatively short plugs were found to be stable, but the maximum length of stable plugs was shown to increase with decreasing fluid viscosity, reaching lengths comparable to the tube radius.

A decrease in propagation speed usually causes a decrease in the deposited film thickness (Han & Shikazono 2009), and Fujioka et al.'s (2008) 2D simulations of plug propagation in rigid channels showed that this effect accelerates the plugs' evolution toward rupture: If an unstable plug deposits more fluid than it accumulates, its length decreases continuously, creating an increase in the driving pressure gradient, which increases its velocity and thus the deposited film thickness yet further, leading to a further increase in the rate at which fluid is lost from the plug. Conversely, an increase in plug length above its equilibrium value reduces the driving pressure gradient and leads to slower plug propagation and a thinner deposited film, increasing the rate at which the plug accumulates fluid. This implies that for a given pressure drop and film height ahead of the plug there exists a critical length (corresponding to the steady state) above which the propagating plug will not rupture but will continue to accumulate fluid, which may be advantageous for drug-delivery and surfactant replacement applications.

Zheng et al. (2009b) considered the effect of wall elasticity on the propagation of liquid plugs, using an experimental analog of the 2D Starling resistor comprising a square PDMS microchannel (100 μm × 100 μm cross section) in which one wall is sufficiently thin that it behaves as an elastic membrane. The deformation induced by steadily propagating plugs and the driving pressure drop as a function of propagation speed were both found to be in qualitative agreement with their 2D computations. Compared to rigid channels, a smaller pressure drop was required to drive a plug of fixed length at a given speed, a result also found by Howell et al. (2000) in their theoretical study of slowly propagating long plugs in axisymmetric tubes. Zheng et al.'s (2009b) computations also showed that wall stresses and stress gradients are minimized in slightly compliant channels, but that the significant membrane deformations in more compliant channels can lead to peak stress values greater than those in rigid channels, a result suggesting that the already weakened airways of patients suffering from emphysema may be susceptible to further damage due to the stresses induced by propagating occlusions during mechanical ventilation. Investigations into the behavior of nonaxisymmetric plugs in buckled elastic tubes and their stability have not yet been conducted and represent a fruitful area for future studies.

If the plug is sufficiently long, so that there is little interaction between its front and rear interfaces, or if airway closure leads to a complete collapse of the airway, the rear interface behaves as though it were propagating into a completely fluid-filled system, which describes the state of the lungs before the first breath is taken.

4.3. Airway Reopening

In newborn infants, the lungs are completely filled with fluid that must be rapidly cleared before gas exchange can take place (Bland 2001, Te Pas et al. 2008). The exact volume of fluid present in the lungs immediately after birth is controversial. It is generally agreed that a large volume of fluid is lost during labor (Berger et al. 1998), but some studies find that the volume already decreases in late gestation before the onset of labor (Pfister et al. 2001), whereas others do not (Lines et al. 1997). The discrepancy may result from methodological differences (Pfister et al. 2003), but the subject remains contentious. Phase contrast X-ray imaging of the lungs of rabbits born by Caesarean section has shown that an air-liquid interface progresses rapidly through the airways during inspiratory maneuvers only (Hooper et al. 2007), accompanied by an increase in total lung volume (Siew et al. 2009). The fact that similar patterns were observed when ventilating

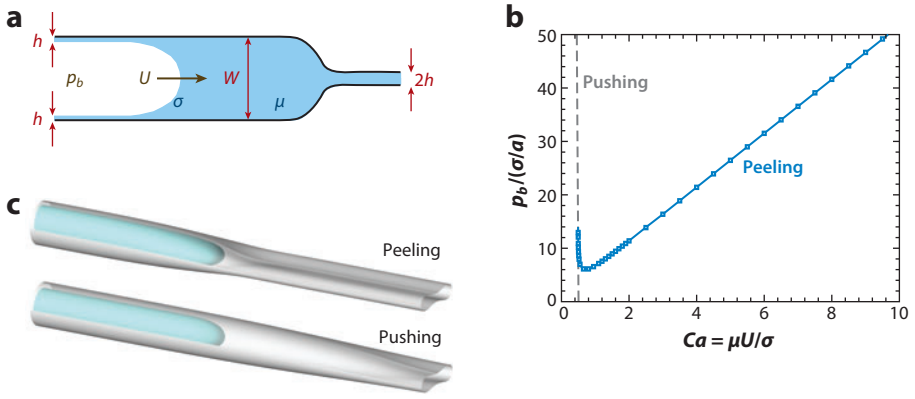

Figure 3

(*a*) Sketch of Gaver et al.'s (1990) model of pulmonary airway reopening. An air finger propagates steadily into a collapsed, elastic tube (or a 2D channel) that is filled with viscous fluid of viscosity μ and surface tension σ. The propagating finger opens the airway and redistributes the fluid into a thin liquid lining. (*b*) Typical pressure flow relationship, showing the pressure p_b required to drive the finger with a given speed U into a collapsed 3D tube of undeformed radius a. The dashed line shows Hazel & Heil's (2003b) asymptotic prediction for the behavior on the low-speed pushing branch. (*c*) Representative shapes of the tube wall and air-liquid interface in the peeling and pushing regimes.

dead newborn rabbits indicates that postbirth liquid clearance does not require any biologically active transport mechanisms (Hooper et al. 2007).

A simple model of airway (re)opening, introduced by Gaver et al. (1990), considers the propagation of an air finger into a uniformly collapsed, fluid-filled tube (or channel), as sketched in **Figure 3*a***. As the finger propagates, the airway's cross-sectional area increases, and fluid is redistributed into a wall-lining layer surrounding the air core. Siew et al. (2009) argued that the volume of liquid within the lungs is too great to be redistributed in this manner, a tacit assumption being that the airways are initially uncollapsed, so that a significant increase in their diameter would be required to accommodate the propagating air finger. They suggested that fluid is instead driven through the airway walls by hydrostatic pressure before being cleared by the lymphatic system and blood vessels. However, estimates provided in their paper indicate that a very large clearance rate would be required (approximately "1,000 times greater than liquid reabsorption rates measured during high-dose adrenaline infusion") and that an unspecified mechanism must retain water in the interstitial tissue until lymphatic clearance. We therefore suggest that airway (re)opening is likely to involve two separate stages: the rapid propagation of an air finger into the initially collapsed airway, during which the volume of the air finger is accommodated by the expansion of the airway to its undeformed (or slightly inflated) state, followed by the removal of liquid through the airway walls on a slower timescale.

Theoretical analyses of the model system in two (Gaver et al. 1996) and three (Hazel & Heil 2002) dimensions revealed that, in the absence of gravitational effects, the relationship between the air pressure in the propagating finger, p_b, and the steady propagation speed, U, has a generic two-branch behavior (see **Figure 3*b***). For sufficiently high propagation speeds, an increase in pressure is required for a further increase in speed, as observed in bench-top experiments (Gaver et al. 1990, Juel & Heap 2007), and the air-liquid interface remains close to the tube walls, peeling them apart. At low speeds, the models predict that a large volume of fluid is pushed ahead of the finger tip, and a decrease in speed is accompanied by an increase in pressure. **Figure 3*c*** shows

representative plots of the system in the pushing and peeling regimes. Gaver et al. (1996) provided a simple explanation for the counterintuitive behavior in the pushing regime for the 2D system, shown in **Figure 3*a***. The air finger propagates into an elastic-walled channel, initially filled with fluid of viscosity μ and surface tension σ, and collapsed to a width of $2h$ far ahead of the finger tip. A decrease in propagation speed U reduces the relative film thickness h/W far behind the finger tip because $h/W \to 0$ when $Ca = \mu U/\sigma \to 0$ (Bretherton 1961), a consequence of the finger tip approaching its static equilibrium configuration: a semicircular interface spanning the entire channel width. However, conservation of mass requires that the film thickness h remains constant, implying that the channel must expand rapidly, $W \to \infty$ as $Ca \to 0$, via an increase in p_b. Hazel & Heil (2003b) realized that this explanation also applies in three dimensions and used it as the basis for a simplified model of the $p_b(Ca)$ curve at small propagation speeds. The model was found to be in good agreement with the results of direct numerical simulations, as shown in **Figure 3*b***.

The pushing and peeling branches are connected at $p_b^{\min}$, the minimum pressure required to achieve steady propagation, which occurs at a finite speed. Hazel & Heil (2003b) showed that if the initial level of collapse of the tube is increased, $p_b^{\min}$ decreases because a smaller volume of fluid is redistributed per unit time with consequent reduced viscous dissipation. Hence, it is mechanically advantageous for the lungs to be as collapsed as possible before the first breath is taken, a result supported by observations that postnatal gas exchange in lambs is enhanced by a reduction in lung liquid volume (Berger et al. 1996). For sufficiently collapsed tubes the reopening air pressures can even be lower than the external pressure (Hazel & Heil 2003b, Heap & Juel 2009), indicating that steady propagation can occur without fully reopening the airway. Negative intrapulmonary pressures have indeed been measured in advanced labor (Pfister et al. 2001), providing further evidence that the lungs are collapsed at birth.

For strongly collapsed tubes a number of different reopening regimes have been observed experimentally (Heap & Juel 2008, 2009). The air finger takes different shapes as the level of collapse increases, progressing from symmetric, to asymmetric, to double-tipped and finally to a pointed configuration in which the curvature is reversed over a portion of the tip. The pointed configuration was found to propagate very rapidly at a low pressure, so it may be beneficial to operate in this regime when attempting to rapidly reopen collapsed airways while avoiding damage to the airway tissue. A theoretical explanation for the existence of these shapes and predictions of their ranges of existence and stability are not yet available, although double-tipped static menisci have been found to exist in sufficiently collapsed elastic tubes (Heil 1999) and channels (van Honschoten et al. 2009).

The theoretical models' predicted increase in driving pressure at low speeds has never been observed in experiments, and indeed Halpern et al. (2005) showed that steady motion on the pushing branch is unstable in the 2D model. If the driving pressure is held constant, the system either evolves toward the corresponding solution on the peeling branch, or the air finger slows down indefinitely. For controlled perturbations to a fixed volume flux, the system exhibits relaxation oscillations, switching between low speed to high speed in a stick-slip-like behavior. Hence, steady propagation at low speeds is not possible in these models, suggesting that airway reopening may be an intrinsically unsteady phenomenon.

However, an additional mechanism that can alter the low-speed behavior is transverse gravity and the consequent buoyant rise of the air finger. The explanation for the development of the pushing branch given above relied crucially on the fact that $h/W \to 0$ when the system approaches its static equilibrium configuration as $Ca \to 0$. Jensen et al. (1987) demonstrated that in the presence of transverse gravity, there exist static equilibrium configurations in which a finite layer of fluid remains on the lower wall. Such configurations exist when the hydrostatic pressure drop through the fluid over the channel half-width is greater than the pressure jump across the

corresponding interface in the absence of gravity. Increasing the channel width increases the hydrostatic pressure drop, but reduces the interface curvature and, hence, the interfacial pressure jump. Thus, no matter how weak the gravitational force, for a sufficiently wide channel, there will be a static equilibrium in which a fluid film of finite thickness remains below the air finger. Hence it is possible for the system to approach a static solution as $Ca \to 0$ and conserve mass without the channel having to expand indefinitely, allowing p_b to remain finite. This was confirmed in Hazel & Heil's (2008) 2D computations showing that for parameters corresponding to Gaver et al.'s (1990) experiments, the p_b-U curve can remain monotonic. The same mechanism is expected to apply in three dimensions, and significant buoyant rise has been observed in experiments (Juel & Heap 2007). In the presence of transverse gravity, steady propagation is therefore possible at low speeds and low pressures.

We have already indicated that fluid-mechanical stresses may contribute to ventilator-induced lung injury when patients are subjected to artificial ventilation. Although the relative importance of this effect, relative to so-called barotrauma (or volutrauma), caused by the overinflation of the lungs, is still being debated in the literature (see, e.g., Ricard et al. 2003), cell culture studies by Bilek et al. (2003) and Kay et al. (2004) have shown that the fluid stresses generated by propagating air fingers can be large enough to damage the epithelial cells that line the airway wall. Motivated by this observation, Jacob & Gaver (2005) computed the stresses on the epithelial cells, assuming them to be rigid. The actual flow-induced deformation of the epithelium was considered by Naire & Jensen (2005), who treated it as a continuous elastic surface layer. Their study confirmed Bilek et al.'s (2003) observation that the presence of surfactant can lead to a dramatic reduction in the fluid stresses acting on the epithelial cells. More recently, Dailey et al. (2007, 2009) performed more detailed simulations in which they analyzed the flow-induced deformation of individual epithelial cells.

5. CONCLUSIONS AND PERSPECTIVES

The majority of studies reviewed above are concerned with idealized model problems, with our main aim having been to describe progress in the understanding of fundamental mechanisms. In specific physiological applications, these mechanisms will be modified by the many additional effects ignored in the idealized models. For instance, collapsible vessels in the human body have more complicated geometries and constitutive properties than the thin-walled, homogeneous tubes typically considered in studies of the Starling resistor. However, Yang et al.'s (2009) studies of airway collapse, using a multigeneration airway model, show that the collapse pattern is similar to that predicted by models based on the Starling resistor. Similarly, the basic instability mechanism responsible for flow-induced compression of stenosed arteries was originally investigated with a Starling-resistor-like setup by Tang et al. (1999). The mechanism thus identified has since been shown to describe the behavior of more realistic models in which the geometry and composition of the stenosed vessel are obtained directly from MRI scans (Tang et al. 2009). Another example concerns the recent advances in modeling cerebrospinal fluid dynamics in the brain with the aim of understanding hydrocephalus, or water on the brain. The predictions of simple 1D collapsible-tube theory (Linninger et al. 2005) and axisymmetric poroelastic models (Smillie et al. 2005) that the rise in intracranial pressure is not causal, but a consequence of impaired absorption of fluid, have been confirmed, again using anatomically realistic geometries, in simulations of fluid flow coupled to poroelasticity (Linninger et al. 2009).

The close coupling between medical imaging, computational simulations, and clinical diagnosis is a rapidly growing trend, as demonstrated in the recent reviews by Taylor & Figueroa (2009) and Taylor & Steinman (2010), who also provide overviews of the different numerical algorithms for

physiological fluid-structure-interaction problems. The trend is strengthened by the accessibility of freely available tools for mesh generation from medical-image data (e.g., Antiga et al.'s (2008) Vascular Modeling Toolkit) and the fact that an increasing number of commercial and open-source software packages provide fluid-structure-interaction capabilities. One of the main difficulties for accurate patient-specific simulation of physiological fluid-structure interaction problems is likely to remain the in vivo determination of the tissues' constitutive properties.

Nonetheless, the ever-increasing complexity of patient-specific studies means that results become harder to interpret. It is our belief that such interpretation relies on the fundamental understanding of physiological fluid-structure interaction gained from the types of idealized models described above, which makes their study as important as ever.

DISCLOSURE STATEMENT

The authors are not aware of any affiliations, memberships, funding, or financial holdings that might be perceived as affecting the objectivity of this review.

ACKNOWLEDGMENTS

We would like to acknowledge helpful discussions with Chris Bertram, Patrick Hurley, Oliver Jensen, and Chris Johnson.

LITERATURE CITED

Alipour F, Berry DA, Titze IR. 2000. A finite-element model of vocal-fold vibration. *J. Acoust. Soc. Am.* 108:3003–12

Alipour F, Scherer RC. 2000. Vocal fold bulging effects on phonation using a biophysical computer model. *J. Voice* 14:470–83

Antiga L, Piccinelli M, Botti L, Ene-Iordache B, Remuzzi A, Steinman DA. 2008. An image-based modeling framework for patient-specific computational hemodynamics. *Med. Biol. Eng. Comput.* 46:1097–112

Berger PJ, Kyriakides MA, Smolich JJ, Ramsden CA, Walker AM. 1998. Massive decline in lung liquid before vaginal delivery at term in the fetal lamb. *Am. J. Obstet. Gynecol.* 178:223–27

Berger PJ, Smolich JJ, Ramsden CA, Walker AM. 1996. Effect of lung liquid volume on respiratory performance after Caesarean delivery in the lamb. *J. Physiol.* 492:905–12

Berry DA, Herzel H, Titze IR, Krischer K. 1994. Interpretation of biomechanical simulations of normal and chaotic vocal fold oscillations with empirical eigenfunctions. *J. Acoust. Soc. Am.* 95:3595–604

Berry DA, Titze IR. 1996. Normal modes in a continuum model of vocal fold tissues. *J. Acoust. Soc. Am.* 100:3345–54

Bertram CD. 2003. Experimental studies of collapsible tubes. See Pedley & Carpenter 2003, pp. 51–65

Bertram CD. 2008. Flow-induced oscillation of collapsed tubes and airway structures. *Respir. Physiol. Neurobiol.* 163:256–65

Bertram CD, Godbole SA. 1997. LDA measurements of velocities in a simulated collapsed tube. *J. Biomech. Eng.* 119:357–63

Bertram CD, Muller M, Ramus F, Nugent AH. 2001. Measurements of steady turbulent flow through a rigid simulated collapsed tube. *Med. Biol. Eng. Comput.* 39:422–27

Bertram CD, Nugent AH. 2005. The flow field downstream of an oscillating collapsed tube. *J. Biomech. Eng.* 127:39–45

Bertram CD, Raymond CJ, Pedley TJ. 1990. Mapping of instabilities for flow through collapsible tubes of differing length. *J. Fluids Struct.* 4:125–53

Bertram CD, Truong N, Hall SD. 2007. Design of PIV experiments on collapsible-tube oscillation onset, to match numerical simulations. In *Proc. 19th Bioeng. Conf.*, ed. T Yamaguchi, pp. 5–6. Sendai: Jpn. Soc. Mech. Eng.

Bertram CD, Truong N, Hall SD. 2008. PIV measurements of the flow field just downstream of an oscillating collapsible tube. *J. Biomech. Eng.* 130:061011
Bertram CD, Tscherry J. 2006. The onset of flow-rate limitation and flow-induced oscillations in collapsible tubes. *J. Fluids Struct.* 22:1029–45
Bilek AM, Dee KC, Gaver DP III. 2003. Mechanisms of surface-tension-induced epithelial cell damage in a model of pulmonary airway reopening. *J. Appl. Physiol.* 94:770–83
Bland RD. 2001. Loss of liquid from the lung lumen in labor: more than a simple "squeeze". *Am. J. Physiol. Lung Cell Mol. Physiol.* 280:L602–5
Bretherton FP. 1961. The motion of long bubbles in tubes. *J. Fluid Mech.* 10:166–88
Bull JL, Reickert CA, Tredici S, Komori E, Frank EL, et al. 2005. Flow limitation in liquid-filled lungs: effects of liquid properties. *J. Biomech. Eng.* 127:630–36
Burger EJ Jr, Macklem P. 1968. Airway closure: demonstration by breathing 100% O_2 at low lung volumes and by N_2 washout. *J. Appl. Physiol.* 25:139–48
Burgmann S, Grosse S, Schroder W, Roggenkamp J, Jansen S, et al. 2009. A refractive index-matched facility for fluid-structure interaction studies of pulsatile and oscillating flow in elastic vessels of adjustable compliance. *Exp. Fluids* 47:865–81
Campana DM, Ubal S, Giavedoni MD, Saita FA. 2007. Stability of the steady motion of a liquid plug in a capillary tube. *Ind. Eng. Chem. Res.* 46:1803–9
Cancelli C, Pedley TJ. 1985. A separated-flow model for collapsible-tube oscillations. *J. Fluid Mech.* 157:375–404
Carpenter PW, Garrad AD. 1985. The hydrodynamic instability of flow over Kramer-type compliant surfaces. Part 1. Tollmien-Schlichting instabilities. *J. Fluid Mech.* 155:465–510
Carpenter PW, Garrad AD. 1986. The hydrodynamic instability of flow over Kramer-type compliant surfaces. Part 2. Flow-induced surface instabilities. *J. Fluid Mech.* 170:199–232
Cook DD, Mongeau L. 2007. Sensitivity of a continuum vocal fold model to geometric parameters, constraints, and boundary conditions. *J. Acoust. Soc. Am.* 121:2247–53
Dailey HL, Ricles LM, Yalcin HC, Ghadiali SN. 2009. Image-based finite element modeling of alveolar epithelial cell injury during airway reopening. *J. Appl. Physiol.* 106:221–32
Dailey HL, Yalcin HC, Ghadiali SN. 2007. Fluid-structure modeling of flow-induced alveolar epithelial cell deformation. *Comput. Struct.* 85:1066–71
Dasi LP, Simon HA, Sucoskky P, Yoganathan AP. 2009. Fluid mechanics of artificial heart valves. *Clin. Exp. Pharmacol. Physiol.* 36:225–37
Davies C. 2003. Convective and absolute instabilities of flow over compliant walls. See Pedley & Carpenter 2003, pp. 69–93
Dejonckere P, Lebacq J. 1981. Mechanism of initiation of oscillatory motion in human glottis. *Arch. Int. Physiol. Biochim.* 89:127–36
de Oliveira Rosa M, Pereira JC, Grellet M, Alwan A. 2003. A contribution to simulating a three-dimensional larynx model using the finite-element method. *J. Acoust. Soc. Am.* 114:2893–905
Doare O, de Langre E. 2004. Local and global instability of fluid-conveying pipes on elastic foundations. *J. Fluids Struct.* 16:1–14
Doare O, de Langre E. 2006. The role of boundary conditions in the instability of one-dimensional systems. *Eur. J. Mech. B Fluids* 25:948–59
Duclaux V, Clanet C, Quéré D. 2006. The effects of gravity on the capillary instability in tubes. *J. Fluid Mech.* 556:217–26
Fujioka H, Grotberg JB. 2004. Steady propagation of a liquid plug in a two-dimensional channel. *J. Biomech. Eng.* 126:567–77
Fujioka H, Takayama S, Grotberg JB. 2008. Unsteady propagation of a liquid plug in a liquid-lined straight tube. *Phys. Fluids* 20:062104
Fullana JM, Zaleski S. 2009. A branched one-dimensional model of vessel networks. *J. Fluid Mech.* 621:183–204
Gaver DP III, Halpern D, Jensen OE, Grotberg JB. 1996. The steady motion of a semi-infinite bubble through a flexible walled channel. *J. Fluid Mech.* 319:25–56
Gaver DP III, Samsel RW, Solway J. 1990. Effects of surface tension and viscosity on airway reopening. *J. Appl. Physiol.* 369:74–85

Grotberg JB, Jensen OE. 2004. Biofluid mechanics in flexible tubes. *Annu. Rev. Fluid Mech.* 36:121–47
Gunter HE. 2003. A mechanical model of vocal-fold collision with high spatial and temporal resolution. *J. Acoust. Soc. Am.* 113:994–1000
Halpern D, Naire S, Jensen OE, Gaver DP. 2005. Unsteady bubble propagation in a flexible channel: predictions of a viscous stick-slip instability. *J. Fluid Mech.* 528:53–86
Han Y, Shikazono N. 2009. Measurement of the liquid film thickness in micro tube slug flow. *Int. J. Heat Fluid Flow* 30:842–53
Hazel AL, Heil M. 2002. The steady propagation of a semi-infinite bubble into a tube of elliptical or rectangular cross-section. *J. Fluid Mech.* 470:91–114
Hazel AL, Heil M. 2003a. Steady finite Reynolds number flow in three-dimensional collapsible tubes. *J. Fluid Mech.* 486:79–103
Hazel AL, Heil M. 2003b. Three-dimensional airway reopening: the steady propagation of a semi-infinite bubble into a buckled elastic tube. *J. Fluid Mech.* 478:47–70
Hazel AL, Heil M. 2005. Surface-tension-induced buckling of liquid-lined elastic tubes: a model for pulmonary airway closure. *Proc. R. Soc. A* 461:1847–68
Hazel AL, Heil M. 2008. The influence of gravity on the steady propagation of a semi-infinite bubble into a flexible channel. *Phys. Fluids* 20:092109
Heap A, Juel A. 2008. Anomalous bubble propagation in elastic tubes. *Phys. Fluids* 20:081702
Heap A, Juel A. 2009. Bubble transitions in strongly collapsed tubes. *J. Fluid Mech.* 633:485–507
Heil M. 1999. Minimal liquid bridges in non-axisymmetrically buckled elastic tubes. *J. Fluid Mech.* 380:309–37
Heil M, Boyle J. 2010. Self-excited oscillations in three-dimensional collapsible tubes: simulating their onset and large-amplitude oscillations. *J. Fluid Mech.* 652:405–26
Heil M, Hazel AL, Smith JA. 2008. The mechanics of airway closure. *Respir. Physiol. Neurobiol.* 163:214–21
Heil M, Jensen OE. 2003. Flows in deformable tubes and channels: theoretical models and biological applications. See Pedley & Carpenter 2003, pp. 15–49
Heil M, Waters SL. 2006. Transverse flows in rapidly oscillating, elastic cylindrical shells. *J. Fluid Mech.* 547:185–214
Heil M, Waters SL. 2008. How rapidly oscillating collapsible tubes extract energy from a viscous mean flow. *J. Fluid Mech.* 601:199–227
Hills BA. 1999. An alternative view of the role(s) of surfactant and the alveolar model. *J. Appl. Physiol.* 87:1567–83
Hoepffner J, Bottaro A, Favier J. 2010. Mechanisms of non-modal energy amplification in channel flow between compliant walls. *J. Fluid Mech.* 642:489–507
Hooper SB, Kitchen MJ, Wallace MJ, Yagi N, Uesugi K, et al. 2007. Imaging lung aeration and lung liquid clearance at birth. *FASEB J.* 21:3329–37
Howell PD, Waters SL, Grotberg JB. 2000. The propagation of a liquid bolus along a liquid-lined flexible tube. *J. Fluid Mech.* 406:309–35
Humphrey JD, Taylor CA. 2008. Intracranial and abodominal aortic aneurysms: similarities, differences, and need for a new class of computational models. *Annu. Rev. Biomed. Eng.* 10:221–46
Hunter EJ, Titze IR, Alipour F. 2004. A three-dimensional model of vocal fold abduction/adduction. *J. Acoust. Soc. Am.* 115:1474–759
Ishizaka K, Flanagan JL. 1972. Synthesis of voiced sounds from a two-mass model of the vocal cords. *Bell Syst. Technol. J.* 51:1233–67
Jacob AM, Gaver DP. 2005. An investigation of the influence of cell topography on epithelial mechanical stresses during pulmonary airway reopening. *Phys. Fluids* 17:031502
Jensen MH, Libchaber A, Pelcé P, Zocchi G. 1987. Effect of gravity on the Saffman-Taylor meniscus: theory and experiment. *Phys. Rev. A* 35:2221–27
Jensen OE. 1997. The thin liquid lining of a weakly curved cylindrical tube. *J. Fluid Mech.* 331:373–403
Jensen OE, Heil M. 2003. High-frequency self-excited oscillations in a collapsible-channel flow. *J. Fluid Mech.* 481:235–68
Jiang JJ, Titze IR. 1994. Measurement of vocal fold intraglottal pressure and impact stress. *J. Voice* 8:132–44
Johnson M, Kamm RD, Ho LW, Shapiro A, Pedley TJ. 1991. The non-linear growth of surface-tension-driven instabilities of a thin annular film. *J. Fluid Mech.* 233:141–56

Juel A, Heap A. 2007. The reopening of a collapsed fluid-filled elastic tube. *J. Fluid Mech.* 572:287–310
Kaneko T, Masuda T, Shimada A, Suzuki H, Hayasaki K, Komatsu K. 1987. Resonance characteristics of the human vocal fold in vivo and in vitro by an impulse excitation. In *Laryngeal Function in Phonation and Respiration*, ed. T Baer, C Sasaki, KS Harris, pp. 349–65. Boston: College Hill
Kay SS, Bilek AM, Dee KC, Gaver DP III. 2004. Pressure gradient, not exposure duration, determines the extent of epithelial cell damage in a model of pulmonary airway reopening. *J. Appl. Physiol.* 97:269–76
Kounanis K, Mathioulakis DS. 1999. Experimental flow study within a self oscillating collapsible tube. *J. Fluids Struct.* 13:61–73
Krane MH. 2005. Aeroacoustic production of low-frequency unvoiced speech sounds. *J. Acoust. Soc. Am.* 118:410–27
Krechetnikov R, Marsden JE. 2007. Dissipation-induced instabilities in finite dimensions. *Rev. Mod. Phys.* 79:519–53
Kucinschi BR, Scherer RC, DeWitt KJ, Ng TTM. 2006. Flow visualization and acoustic consequences of the air moving through a static model of the human larynx. *J. Biomech. Eng.* 128:380–90
Kumaran V. 2003. Hydrodynamic stability of flow through compliant channels and tubes. See Pedley & Carpenter 2003, pp. 95–118
Larose PG, Grotberg JB. 1997. Flutter and long-wave instabilities in compliant channels conveying developing flows. *J. Fluid Mech.* 331:37–58
Lasheras JC. 2007. The biomechanics of arterial aneurysms. *Annu. Rev. Fluid Mech.* 39:293–319
Lindsley WG, Collicott SH, Franz GN, Stolarik B, McKinney W, Frazer DG. 2005. Asymmetric and axisymmetric constant curvature liquid-gas interfaces in pulmonary airways. *Ann. Biomed. Eng.* 33:365–75
Lines A, Hooper SB, Harding R. 1997. Lung liquid production rates and volumes do not decrease before labor in healthy fetal sheep. *J. Appl. Physiol.* 82:927–32
Link G, Kaltenbacher M, Breuer M, Döllinger M. 2009. A 2D finite-element scheme for fluid-solid-acoustic interactions and its application to human phonation. *Comput. Methods Appl. Mech. Eng.* 198:3321–34
Linninger AA, Sweetman B, Penn R. 2009. Normal and hydrocephalic brain dynamics: the role of reduced cerebrospinal fluid reabsorption in ventricular enlargement. *Ann. Biomed. Eng.* 37:1434–47
Linninger AA, Tsakiris C, Zhu DC, Xenos M, Roycewicz P, et al. 2005. Pulsatile cerebrospinal fluid dynamics in the human brain. *IEEE Trans. Biomed. Eng.* 52:557–65
Liu HF, Luo XY, Cai ZX, Pedley TJ. 2009. Sensitivity of unsteady collapsible channel flows to modelling assumptions. *Commun. Numer. Methods Eng.* 25:483–504
Luo H, Mittal R, Zheng X, Bielamowicz SA. 2009. Analysis of flow-structure interaction in the larynx during phonation using an immersed-boundary method. *J. Acoust. Soc. Am.* 126:816–24
Luo H, Mittal R, Zheng X, Bielamowicz SA, Walsh RJ, Hahn JK. 2008a. An immersed-boundary method for flow-structure interaction in biological systems with application to phonation. *J. Comput. Phys.* 227:9303–32
Luo XY, Cai ZX, Li WG, Pedley TJ. 2008b. The cascade structure of linear instability in collapsible channel flows. *J. Fluid Mech.* 600:45–76
Luo XY, Pedley TJ. 1996. A numerical simulation of unsteady flow in a two-dimensional collapsible channel. *J. Fluid Mech.* 314:191–225
Luo XY, Pedley TJ. 1998. The effects of wall inertia on flow in a two-dimensional collapsible channel. *J. Fluid Mech.* 363:253–80
Macklem PT. 1971. Airway obstruction and collateral ventilation. *Physiol. Rev.* 51:368–436
Mandre S, Mahadevan L. 2010. A generalized theory of viscous and inviscid flutter. *Proc. R. Soc. A* 466:141–56
Manuilovich SV. 2004. Propagation of a Tollmien-Schlichting wave over the junction between rigid and compliant surfaces. *Fluid Dyn.* 39:702–17
Marzo A, Luo XY, Bertram CD. 2005. Three-dimensional collapse and steady flow in thick-walled tubes. *J. Fluids Struct.* 20:817–35
McGowan R. 1991. Phonation from a continuum mechanics point of view. In *Vocal Fold Physiology: Acoustic, Perceptual, and Physiological Aspects of Voice Mechanisms*, ed. J Griffin, B Hammarberg, pp. 65–72. San Diego: Singular
McGowan RS. 1988. An aeroacoustic approach to phonation. *J. Acoust. Soc. Am.* 83:696–704

Naire S, Jensen OE. 2005. Epithelial cell deformation during surfactant-mediated airway reopening: a theoretical model. *J. Appl. Physiol.* 99:458–71
Neubauer J, Zhang Z, Miraghaie R, Berry DA. 2007. Coherent structures of the near field flow in a self-oscillating physical model of the vocal folds. *J. Acoust. Soc. Am.* 121:1102–18
Ohba K, Sakurai A, Oka J. 1997. Laser Doppler measurement of local flow field in collapsible tube during self-excited oscillation. *JSME Int. J. Ser. C* 40:665–70
O'Reilly OM, Malhotra NK, Namachchivaya NS. 1996. Some aspects of destabilization in reversible dynamical systems with application to follower forces. *Nonlinear Dyn.* 10:63–87
Pedley TJ, Carpenter PW, eds. 2003. *Flow in Collapsible Tubes and Past Other Highly Compliant Boundaries*. Dordrecht: Kluwer
Pedley TJ, Luo XY. 1998. Modelling flow and oscillations in collapsible tubes. *Theor. Comput. Fluid Dyn.* 10:277–94
Pedley TJ, Stephanoff KD. 1985. Flow along a channel with a time-dependent indentation in one wall: the generation of vorticity waves. *J. Fluid Mech.* 160:337–67
Pfister RE, Kyriakides MA, Berger PJ, Ramsden CA, Cassin RS, Perks AM. 2003. Letters to the editor. *J. Appl. Physiol.* 94:1293–94
Pfister RE, Ramsden CA, Neil HL, Kyriakides MA, Berger PJ. 2001. Volume and secretion rate of lung liquid in the final days of gestation and labour in the fetal sheep. *J. Physiol.* 535:889–99
Popel AS, Johnson PC. 2005. Microcirculation and hemorheology. *Annu. Rev. Fluid Mech.* 37:43–69
Ricard JD, Dreyfuss D, Saumon G. 2003. Ventilator-induced lung injury. *Eur. Respir. J.* 22(Suppl.):S2–9
Rosenfeld M. 1995. A numerical study of pulsating flow behind a constriction. *J. Fluid Mech.* 301:203–23
Sera T, Yokota H, Fujisaki K, Fukasaku K, Tachibana H, et al. 2008. Development of high-resolution 4D in vivo-CT for visualization of cardiac and respiratory deformations of small animals. *Phys. Med. Biol.* 53:4285–301
Sforza DM, Putman CM, Cebral JR. 2009. Hemodynamics of cerebral aneurysms. *Annu. Rev. Fluid Mech.* 41:91–107
Shankar V, Kumaran V. 2000. Stability of fluid flow in a flexible tube to non-axisymmetric disturbances. *J. Fluid Mech.* 407:291–314
Siew ML, Wallace MJ, Kitchen MJ, Lewis RA, Fouras A, et al. 2009. Inspiration regulates the rate and temporal pattern of lung liquid clearance and lung aeration at birth. *J. Appl. Physiol.* 106:1888–95
Sirovich L. 1987. Turbulence and the dynamics of coherent structures. Parts I–III. *Q. Appl. Math.* 45:561–90
Smillie A, Sobey I, Molnar Z. 2005. A hydroelastic model of hydrocephalus. *J. Fluid Mech.* 539:417–43
Stewart PS, Heil M, Waters SL, Jensen OE. 2010. Sloshing and slamming oscillations in collapsible channel flow. *J. Fluid Mech.* In press
Stewart PS, Waters SL, Jensen OE. 2009. Local and global instabilities of flow in a flexible-walled channel. *Eur. J. Mech. B Fluids* 28:541–57
Tang D, Yang C, Kobayashi S, Zheng J, Woodard PK, et al. 2009. 3D MRI-based anisotropic FSI models with cyclic bending for human coronary atherosclerotic plaque mechanical analysis. *J. Biomech. Eng.* 131:061010
Tang D, Yang J, Yang C, Ku DN. 1999. A nonlinear axisymmetric model with fluid-wall interactions for steady viscous flow in stenotic elastic tubes. *J. Biomech. Eng.* 121:494–501
Tao C, Jiang JJ. 2007. Mechanical stress during phonation in a self-oscillating finite-element vocal fold model. *J. Biomech.* 40:2191–98
Tao C, Jiang JJ, Zhang Y. 2006. Simulation of vocal fold impact pressures with a self-oscillating finite-element model. *J. Acoust. Soc. Am.* 119:3987–94
Taylor CA, Figueroa CA. 2009. Patient-specific modeling of cardiovascular mechanics. *Annu. Rev. Biomed. Eng.* 11:109–34
Taylor CA, Steinman DA. 2010. Image-based modeling of blood flow and vessel wall dynamics: applications, methods and future directions. *Ann. Biomed. Eng.* 38:1188–203
Te Pas AB, Davis PG, Hooper SB, Morley CJ. 2008. From liquid to air: breathing after birth. *J. Pediatr.* 152:607–11
Thomson SL, Mongeau L, Frankel SH. 2005. Aerodynamic transfer of energy to the vocal folds. *J. Acoust. Soc. Am.* 118:1689–700

Thomson SL, Mongeau L, Frankel SH. 2007. Flow over a membrane-covered, fluid-filled cavity. *Comput. Struct.* 85:1012–19

Titze IR. 1973. The human vocal cords: a mathematical model. Part I. *Phonetica* 28:129–70

Titze IR. 1988. The physics of small-amplitude oscillation of the vocal folds. *J. Acoust. Soc. Am.* 83:1536–52

Titze IR, Schmidt SS, Titze MR. 1995. Phonation threshold pressure in a physical model of the vocal fold mucosa. *J. Acoust. Soc. Am.* 97:3080–84

Titze IR, Strong WJ. 1975. Normal modes in vocal cord tissues. *J. Acoust. Soc. Am.* 57:736–44

Triep M, Brücker C, Schröder W. 2005. High-speed PIV measurements of the flow downstream of a dynamic mechanical model of the human vocal folds. *Exp. Fluids* 39:232–45

Truong NK, Bertram CD. 2009. The flow-field downstream of a collapsible tube during oscillation onset. *Commun. Numer. Methods Eng.* 25:405–28

Ubal S, Campana DM, Giavedoni MD, Saita FA. 2008. Stability of the steady-state displacement of a liquid plug driven by constant pressure difference along a prewetted capillary tube. *Ind. Eng. Chem. Res.* 47:6307–15

van de Vosse FN, Stergiopulos N. 2011. Pulse wave propagation in the arterial tree. *Annu. Rev. Fluid Mech.* 43:467–99

van der Meer JC. 1990. Hamiltonian Hopf bifurcation with symmetry. *Nonlinearity* 3:1041–56

van Honschoten JW, Escalante M, Tas NR, Elwenspoek M. 2009. Formation of liquid menisci in flexible nanochannels. *J. Colloid Interface Sci.* 329:133–39

Venugopal AM, Quick CM, Laine GA, Stewart RH. 2009. Optimal postnodal lymphatic network structure that maximizes active propulsion of lymph. *Am. J. Physiol. Heart Circ. Physiol.* 296:H303–9

Wang JW, Chew YT, Low HT. 2009. Effects of downstream system of self-excited oscillations in collapsible tubes. *Commun. Numer. Methods Eng.* 25:429–45

Weaver D, Païdoussis M. 1977. On the collapse and flutter phenomena in thin tubes conveying fluid. *J. Sound Vib.* 50:117–32

Weinberg EJ, Shahmirzadi D, Mofrad MRK. 2010. On the multiscale modeling of heart valve biomechanics in health and disease. *Biomech. Model. Mechanobiol.* 9:373–87

Whittaker RJ, Heil M, Jensen OE, Waters SL. 2010a. Predicting the onset of high-frequency self-excited oscillations in elastic-walled tubes. *Proc. R. Soc. A.* In press; doi:10.1098/rspa.2009.0641

Whittaker RJ, Heil M, Jensen OE, Waters SL. 2010b. A rational derivation of a tube law from shell theory. *Q. J. Mech. Appl. Math.* In press; doi:10.1093/qjmam/hbq020

Whittaker RJ, Waters SL, Jensen OE, Boyle J, Heil M. 2010c. The energetics of flow through a rapidly oscillating tube. Part I: general theory. *J. Fluid Mech.* 648:83–121

Yang XL, Liu Y, Yang JM. 2009. Expiratory flow in a rigid three-generation airway with one collapsible segment. *Commun. Numer. Methods Eng.* 25:553–63

Yasuda T, Okuno T, Yasuda H. 1994. Contact angle of water on polymer surface. *Langmuir* 10:2345–439

Zhang Z. 2008. Influence of flow separation location on phonation onset. *J. Acoust. Soc. Am.* 124:1689–94

Zhang Z. 2009. Characteristics of phonation onset in a two-layer vocal fold model. *J. Acoust. Soc. Am.* 125:1091–102

Zhang Z, Neubauer J, Berry DA. 2007. Physical mechanisms of phonation onset: a linear stability analysis of an aeroelastic continuum model of phonation. *J. Acoust. Soc. Am.* 122:2279–95

Zheng X, Bielamowicz SA, Luo H, Mittal R. 2009a. A computational study of the effect of false vocal folds on glottal flow and vocal fold vibration during phonation. *Ann. Biomed. Eng.* 37:625–42

Zheng Y, Fujioka H, Bian S, Torisawa Y, Huh D, et al. 2009b. Liquid plug propagation in flexible microchannels: a small airway model. *Phys. Fluids* 21:071903

Zheng Y, Fujioka H, Grotberg JC, Grotberg JB. 2006. Effects of inertia and gravity on liquid plug splitting at a bifurcation. *J. Biomech. Eng.* 128:707–16

Annual Review of
Fluid Mechanics

Volume 43, 2011

Contents

Experimental Studies of Transition to Turbulence in a Pipe
T. Mullin 1

Fish Swimming and Bird/Insect Flight
Theodore Yaotsu Wu 25

Wave Turbulence
Alan C. Newell and Benno Rumpf 59

Transition and Stability of High-Speed Boundary Layers
Alexander Fedorov 79

Fluctuations and Instability in Sedimentation
Élisabeth Guazzelli and John Hinch 97

Shock-Bubble Interactions
Devesh Ranjan, Jason Oakley, and Riccardo Bonazza 117

Fluid-Structure Interaction in Internal Physiological Flows
Matthias Heil and Andrew L. Hazel 141

Numerical Methods for High-Speed Flows
Sergio Pirozzoli 163

Fluid Mechanics of Papermaking
Fredrik Lundell, L. Daniel Söderberg, and P. Henrik Alfredsson 195

Lagrangian Dynamics and Models of the Velocity Gradient Tensor in Turbulent Flows
Charles Meneveau 219

Actuators for Active Flow Control
Louis N. Cattafesta III and Mark Sheplak 247

Fluid Dynamics of Dissolved Polymer Molecules in Confined Geometries
Michael D. Graham 273

Discrete Conservation Properties of Unstructured Mesh Schemes
J. Blair Perot 299

Global Linear Instability
Vassilios Theofilis 319

High–Reynolds Number Wall Turbulence
Alexander J. Smits, Beverley J. McKeon, and Ivan Marusic 353

Scale Interactions in Magnetohydrodynamic Turbulence
Pablo D. Mininni 377

Optical Particle Characterization in Flows
Cameron Tropea 399

Aerodynamic Aspects of Wind Energy Conversion
Jens Nørkær Sørensen 427

Flapping and Bending Bodies Interacting with Fluid Flows
Michael J. Shelley and Jun Zhang 449

Pulse Wave Propagation in the Arterial Tree
Frans N. van de Vosse and Nikos Stergiopulos 467

Mammalian Sperm Motility: Observation and Theory
E.A. Gaffney, H. Gadêlha, D.J. Smith, J.R. Blake, and J.C. Kirkman-Brown 501

Shear-Layer Instabilities: Particle Image Velocimetry Measurements and Implications for Acoustics
Scott C. Morris 529

Rip Currents
Robert A. Dalrymple, Jamie H. MacMahan, Ad J.H.M. Reniers, and Varjola Nelko 551

Planetary Magnetic Fields and Fluid Dynamos
Chris A. Jones 583

Surfactant Effects on Bubble Motion and Bubbly Flows
Shu Takagi and Yoichiro Matsumoto 615

Collective Hydrodynamics of Swimming Microorganisms: Living Fluids
Donald L. Koch and Ganesh Subramanian 637

Aerobreakup of Newtonian and Viscoelastic Liquids
T.G. Theofanous 661

Indexes

Cumulative Index of Contributing Authors, Volumes 1–43 691

Cumulative Index of Chapter Titles, Volumes 1–43 699

Errata

An online log of corrections to *Annual Review of Fluid Mechanics* articles may be found at http://fluid.annualreviews.org/errata.shtml